How to cite: *Angew. Chem. Int. Ed.* **2024**, *63*, e202316720
doi.org/10.1002/anie.202316720

Organic Chemistry

An *N*-Heterocyclic Quinodimethane: A Strong Organic Lewis Base Exhibiting Diradical Reactivity

*Jama Ariai, Maya Ziegler, Christian Würtele, and Urs Gellrich**

Abstract: We report the preparation of a new organic σ-donor with a C_6H_4-linker between an *N*-heterocyclic carbene (NHC) and an exocyclic methylidene group, which we term *N*-heterocyclic quinodimethane (NHQ). The aromatization of the C_6H_4-linker provides a decisive driving force for the reaction of the NHQ with an electrophile and renders the NHQ significantly more basic than analogous NHCs or *N*-heterocyclic olefins (NHOs), as shown by DFT computations and competition experiments. In solution, the NHQ undergoes an unprecedented dehydrogenative head-to-head dimerization by C–C coupling of the methylidene groups. DFT computations indicate that this reaction proceeds via an open-shell singlet pathway revealing the diradical character of the NHQ. The product of this dimerization can be described as conjugated *N*-heterocyclic bis-quinodimethane, which according to cyclic voltammetry is a strong organic reducing agent ($E_{1/2} = -1.71$ V vs. Fc/Fc^+) and exhibits a remarkable small singlet–triplet gap of $\Delta E_{S\rightarrow T} = 4.4$ kcal mol^{-1}.

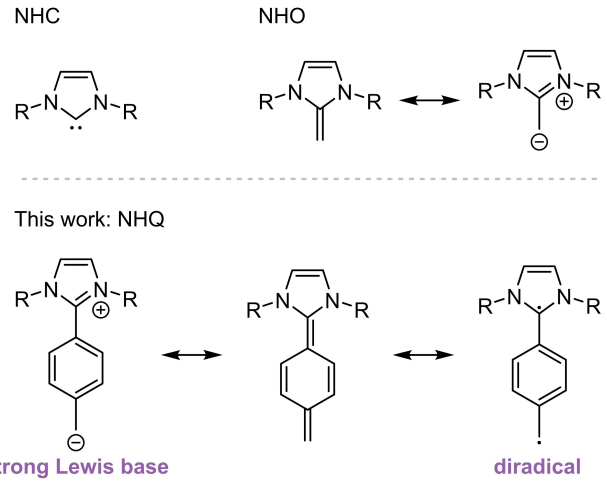

Scheme 1. The concept of this study: The insertion of a C_6H_4-linker between the NHC and the alkylidene group of an NHO should result in an NHQ that is a strong Lewis base with radical reactivity (NHC = *N*-heterocyclic carbene, NHO = *N*-heterocyclic olefin, NHQ = *N*-heterocyclic quinodimethane).

Introduction

N-heterocyclic carbenes (NHCs, Scheme 1, top left), which initially attracted attention as stable representatives of a compound class containing a carbon atom with an electron sextet, have since then found applications as organic σ-donors in catalysis, materials science, and medicine.[1] The extension of NHCs by an alkylidene group leads to *N*-heterocyclic olefins (NHO) that contain a strongly polarized C–C double bond (Scheme 1, top right).[2] When the association of imidazolium-based NHOs with an electrophile leads to aromatization of the *N*-heterocycle, the σ-donor capacity and the relative nucleophilicity of the NHOs exceed that of the corresponding NHCs.[3] In 2020, Hansmann et al. introduced mesoionic NHOs that cannot be described by a charge-neutral Lewis structure and represent the strongest donors and Lewis bases within the class of NHOs.[4] Due to their ability to act as strong σ-donors, NHOs have also been used as ligands in main group chemistry and transition metal catalysis.[5] In addition, their nucleophilicity has been exploited for applications in organocatalysis and polymer chemistry.[6] Furthermore, NHOs bind small molecules such as CO_2 and N_2O.[7] Binding of CO_2 enables its catalytic valorization while the reaction of NHOs with N_2O is of particular interest as it leads to organic super electron donors and diazoolefins. Since aromatization of the imidazoline system during the reaction of the NHO with an electrophile increases the σ-donor strength and the nucleophilicity of the NHO, we expected that a second aromatization would provide an additional driving force to the reaction with an electrophile. This assumption prompted us to investigate an NHO with a C_6H_4-linker between the NHC and the alkylidene group. (Scheme 1, lower panel).

Following the nomenclature of NHCs and NHOs, such a system could be denoted as *N*-heterocyclic quinodimethane (NHQ). Coordination of the NHQ to a Lewis acid (or protonation of the NHQ) would not only lead to aromatiza-

[*] J. Ariai, M. Ziegler, Dr. U. Gellrich
Institut für Organische Chemie, Justus-Liebig-Universität Gießen
Heinrich-Buff-Ring 17, 35392 Gießen (Germany)
E-mail: urs.gellrich@org.chemie.uni-giessen.de
Dr. C. Würtele
Institut für Anorganische und Analytische Chemie, Justus-Liebig-Universität Gießen
Heinrich-Buff-Ring 17, 35392 Gießen (Germany)

tion of the imidazoline ring but also of the C_6H_4-linker. Recent work by Coote, Sherburn and co-workers has confirmed that quinodimethanes (QDMs) exhibit the reactivity of a diradical.[8] Moreover, Ghadwal and co-workers showed that NHC-substituents are well suited to stabilize C-centered radicals.[9] Thus, the question further arises to what extent NHQs might exhibit radical reactivity.

Results and Discussion

We began our study with a computational evaluation of the effects of the C_6H_4-linker on the proton affinity (PA) of NHQ **1** with a Dipp-substituted (Dipp = 2,6-*i*Pr$_2$C$_6$H$_3$) imidazolium backbone, through a comparison to the PAs of NHC **2** and NHO **3**; both of which are iconic examples of their respective compound classes. We chose the ωB97X functional together with the recent D4 correction, a combination which has been shown to be reliable for thermodynamics and kinetics, for this study.[10] For structure optimization, we used the efficient PBEh-3c composite method.[11] The comparison of the computed PAs shows that the PA of **3** is 2.8 kcal mol^{-1} higher than that of **2**. As hypothesized, the incorporation of a C_6H_4-linker at the C2 position has indeed a decisive effect on the basicity of **3**; the PA of NHQ **1** exceeds that of **3** by 22.9 kcal mol^{-1} (Figure 1).

NHQs with phenyl or cyano substituents at the exocyclic ylidene carbon have been reported previously.[12] However, their computed PAs are significantly lower than that of **1** (Figure S15), presumably as a consequence of the –I-effect of these substituents. Encouraged by the computed basicity of **1**, we turned to the synthesis of an imidazolium precursor that would allow us to generate **1** by deprotonation. To this end, imidazolium iodide **4** was synthesized by coupling **2** with 4-iodotoluene according to a procedure described by Ghadwal et al.[13] Treatment of **4** with KHMDS in THF-d_8 resulted in quantitative conversion to **1** (Scheme 2).

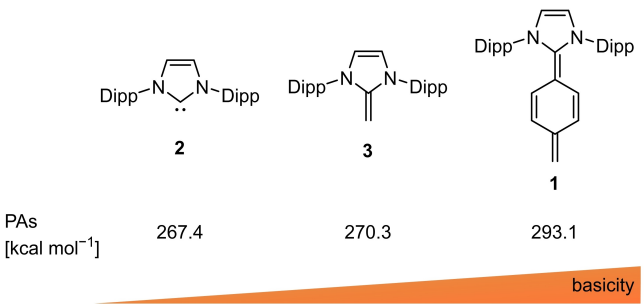

Figure 1. Proton affinities (PAs) of NHQ **1** in comparison to the structurally related NHC **2** and NHO **3** computed at ωB97X-D4/def2-QZVPP//PBEh-3c (Dipp = 2,6-*i*Pr$_2$C$_6$H$_3$).

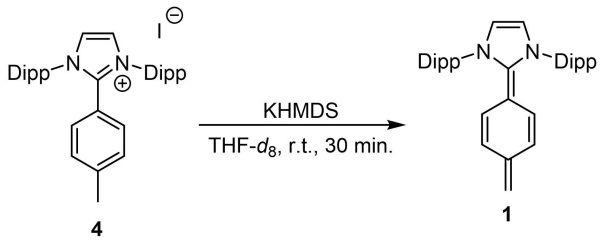

Scheme 2. In situ formation of **1** by deprotonation of **4** with KHMDS.

Diagnostic of the formation of **1** is a pronounced high-field shift in the signals attributable to the C_6H_4-linker in the ^{1}H NMR spectrum, indicating partial de-aromatization and the formation of a quinoidal structure (Figure S26). The CH_2 group appears in the ^{1}H NMR as a singlet at 3.46 ppm. Thus, the signal that can be assigned to this group is slightly low-field shifted compared to the signal of the methylidene group of NHO **3**, but significantly shifted to higher field than the signal of the methylidene group of the parent QDM *p*-xylylene.[14] Likewise, the ^{13}C NMR signal of the CH_2 group at 87.9 ppm is low-field shifted compared to **3** but high-field shifted compared to the signal of the exocyclic carbon of *p*-xylylene. In the course of deprotonation with KHMDS, the color of the reaction mixture turned dark green. UV/Vis spectra of **1** recorded in THF at various concentrations show an intense, sharp absorption band at 330 nm ($\varepsilon = 6.7(2)\cdot10^3$ cm^{-1}M^{-1}) and a broad band of low intensity at about 525 nm ($\varepsilon = 132(5)$ cm^{-1}M^{-1}) (Figure S8). TD-DFT calculations at the ωB97X-D4/def2-QZVPP//PBEh-3c level of theory allowed us to assign the excitation in the UV region to a π→π* transition (computed absorption at 363 nm) from the highest occupied molecular orbital (HOMO) to the lowest unoccupied molecular orbital (LUMO). The broad band in the visible region at 525 nm is almost undetectable when deprotonation is performed with NaHMDS while the HOMO→LUMO transition remains comparable, indicating that the color of the solution is caused by potassium adducts or traces of impurities (Figure S8 and Table S2). The calculations show that the largest coefficient of the HOMO of **1** in the closed-shell singlet state is indeed at the exocyclic methylidene group, as is the spin density of the triplet state of **1** (Figure 2).

We then turned our attention to an experimental assessment of the basicity of **1** by competition experiments. Therefore, imidazolium iodide **5** was added to a solution of **1**, which afforded NHO **3** in near quantitative yield

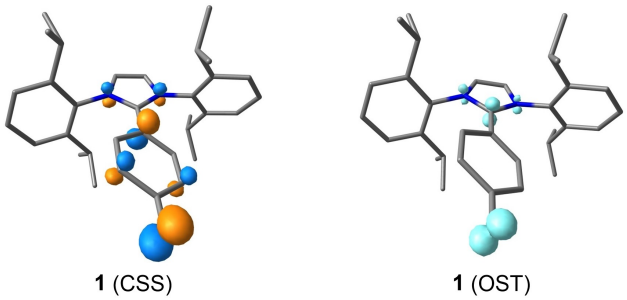

Figure 2. The HOMO of the closed-shell singlet state of **1** (left) and the total spin density of the triplet state of **1** (right). (CSS = closed-shell singlet, OST = open-shell triplet). Hydrogens are omitted for clarity.

supporting the computational result that the PA of NHQ **1** is higher than that of the analogous NHO **3** (Scheme 3).

To explore whether **1** acts not only as Brønsted but also as Lewis base, tris(pentafluoro)phenylborane $B(C_6F_5)_3$ was added to a solution of **1**, which allowed us to isolate the air- and moisture-stable $B(C_6F_5)_3$-adduct **6** in 41 % yield by column chromatography (Scheme 4). NMR analysis of **6** indicates that the formation of the Lewis adduct is accompanied by re-aromatization of the C_6H_4-linker (Figure S36). The C–C bond lengths of the C_6H_4-linker determined by single crystal X-ray diffraction (SCXRD) analysis of **6** support this assumption (Figure 3).[15]

When a THF solution of **1** was exposed to a CO_2-atmosphere, the immediate formation of a precipitate was observed. Filtration and crystallization of the solid from DCM/*n*-hexane allowed us to isolate the carboxylate **7**, which was characterized by NMR, IR, and ESI-MS, in 58 % yield (Scheme 5). The formation of the $B(C_6F_5)_3$-adduct **6** and carboxylate **7** shows that the lifetime of **1** allows its use as a Lewis base. However, attempts to isolate **1** are prevented by its slow conversion to new species in solution. We have followed the progress of this transformation by ^{1}H NMR spectroscopy (Scheme 6).

Already after one day, the appearance of a new set of signals is observed, indicating the emergence of a species with a quinoidal phenylene unit. This is evident from the appearance of two doublets at 5.60 and 5.41 ppm with a coupling constant of 10.3 Hz. In addition, a sharp singlet at 5.03 ppm indicates the formation of a new methylidene group. Within 20 days, the conversion of **1** is complete. When a THF-solution of the new species was overlaid with *n*-pentane and stored at −36 °C for several days, dark orange crystals formed. SCXRD analysis revealed that these crystals consist of the dimer **8**, which was isolated in 36 % yield (Figure 4). Significant alternation of the C–C bond lengths in the C_6H_4-linker of **8** revealed by SCXRD support that **8** is indeed best described as quinoidal structure. The NMR spectrum obtained upon dissolution of the crystals in THF-d_8 proves that the new species into which **1** converts in solution is indeed dimer **8** (Scheme 6). Apparently, **8** is formed by a C–C coupling between the methylidene groups of **1**. This reactivity seems to contradict the ground state polarity of **1**, as two nucleophilic centers react with each

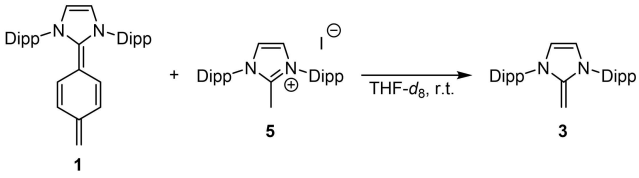

Scheme 3. Deprotonation of imidazolium iodide **5** by NHQ **1**.

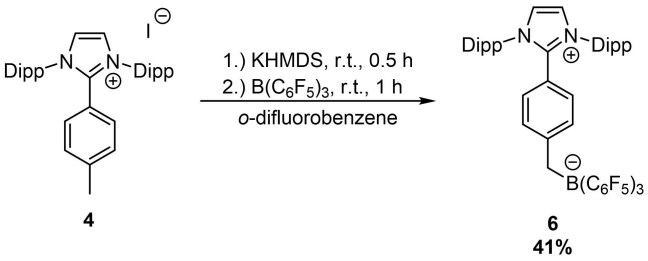

Scheme 4. Synthesis of the NHQ–$B(C_6F_5)_3$-adduct **6**.

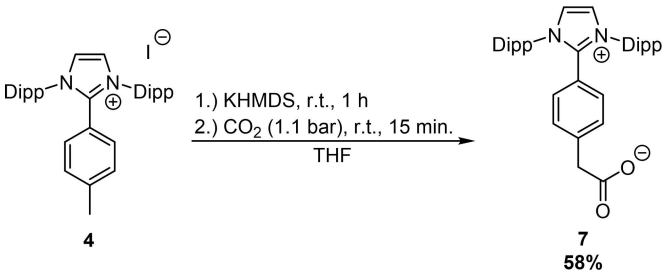

Scheme 5. Synthesis of carboxylate **7** by deprotonation of **4** and exposure to CO_2.

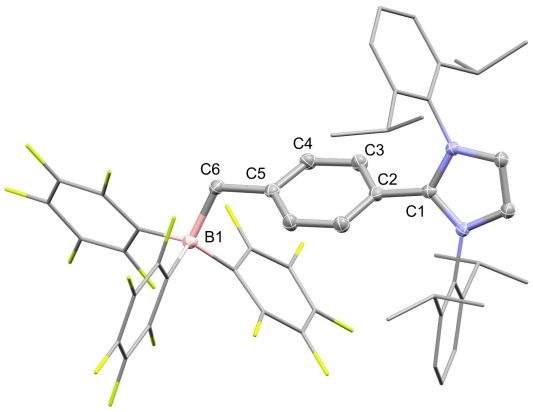

Figure 3. Molecular structure of **6** derived from SCXRD (50% probability ellipsoids, all hydrogens attached to carbons are omitted, Dipp-groups and C_6F_5-rings are shown in stick representation for clarity). Selected bond lengths: C1–C2: 1.466(4) Å, C2–C3: 1.391(4) Å, C3–C4: 1.389(4) Å, C4–C5: 1.401(4) Å, C5–C6: 1.506(4) Å, C6–B1: 1.660(4) Å.

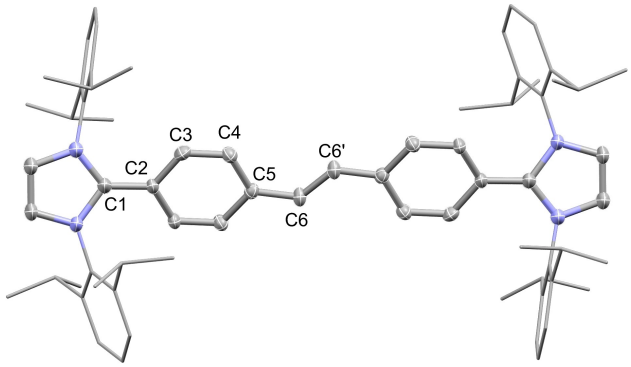

Figure 4. Molecular structure of **8** derived from SCXRD (50% probability ellipsoids, all hydrogens attached to carbons are omitted and Dipp-groups are shown in stick representation for clarity). Selected bond lengths and angles: C1–C2: 1.424(5) Å, C2–C3: 1.420(6) Å, C3–C4: 1.368(6) Å, C4–C5: 1.435(4) Å, C5–C6: 1.397(4) Å, C6–C6′: 1.400(5) Å, C5–C6–C6′: 127.7(3)°.

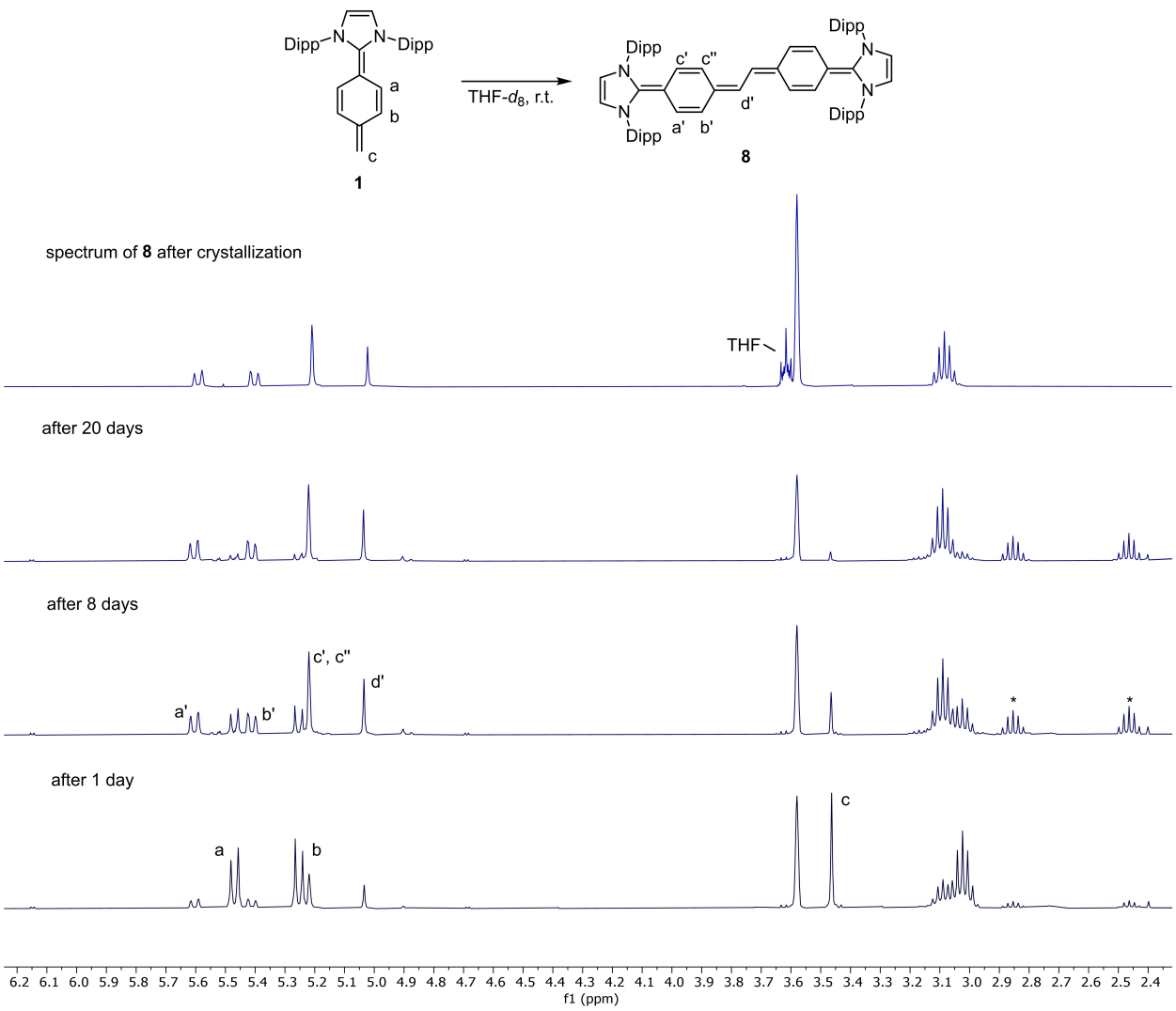

Scheme 6. Monitoring of the conversion of NHQ **1** to dimer **8** by ^{1}H NMR (400 MHz, 0.1 M in THF-d_8) and the ^{1}H NMR spectrum of dimer **8** isolated by crystallization. Signals marked with an asterisk can be assigned to imidazole **10** and 1,3-di(isopropyl)benzene.

other. However, the dimerization of QDMs such as *p*-xylylene is known, and recent computational and experimental studies provided conclusive evidence that this process is initiated by a C–C coupling between the exocyclic methylene carbons along an open-shell diradical pathway.[8,16,14] In addition, the dimerization of heteroatom-containing QDMs has been reported.[17] It is therefore reasonable to attribute the formation of **8** to such diradical coupling as well. We investigated this hypothesis with DFT calculations (Figure 5).

Consistent with the computational study by Sherburn and Coote, dimerization via an open-shell singlet (OSS) state is clearly preferred over the triplet pathway.[8] The calculated barrier of 21.5 kcal mol^{-1} agrees well with the experimental observation that dimerization proceeds, albeit slowly, at r.t. We observed experimentally an acceleration of the formation of **8** at high concentrations (Table S1), which, in agreement with the lack of a detectable intermediate, suggests that the initial C–C coupling is rate-limiting. In the OSS transition state structure, the NHQs are oriented *syn* to each other, presumably due to an attractive dispersive interaction between the bulky Dipp substituents. The product of the coupling, diradical **9**, is more stable in the triplet state, although the energetic preference over the open-shell singlet state is not significant. A feature of NHQ **1** dimerization that distinguishes it from QDM dimerization is that one equivalent of hydrogen is formally released upon formation of **8**. By ^{1}H NMR spectroscopy we observed signals appearing at 2.46 ppm and 2.85 ppm that could be assigned to the formation of by-products during the dimerization of **1**, in a ratio of 1:1 (Scheme 6). From the mother liquor of a crystallization of **8**, we were able to isolate imidazole **10** by column chromatography, thus unambiguously identifying it as one of these by-products. Based on the computational study and the experimental observations, we propose the following mechanism for the formation of dimer **8** and imidazole **10** (Scheme 7): An initial C–C coupling between the methylidene groups of NHQ **1** gives

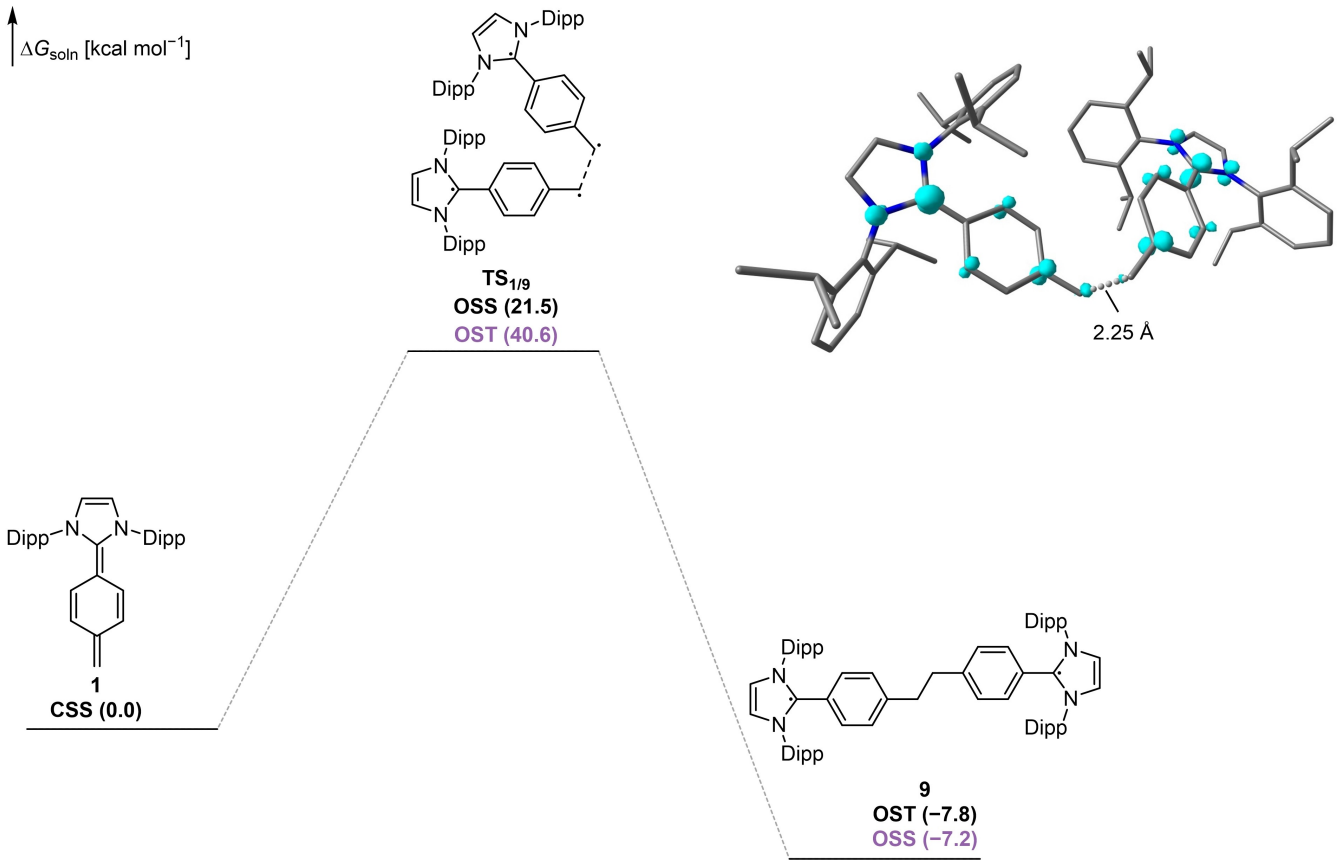

Figure 5. Gibbs free energies for the dimerization of **1** computed at ωB97X-D4/def2-TZVPP//PBEh-3c (CSS = closed-shell singlet, OSS = open-shell singlet, OST = open-shell triplet). Bulk solvation was considered implicitly with the SMD model for THF.[18] The inset shows the open-shell singlet state transition state structure of the C–C bond formation with the spin density.

rise to the diradical **9**. Hydrogen atom transfer (HAT) from diradical **9** to NHQ **1** yields **11** and radical **12**, a reaction that further substantiates the diradical character of **1**. The formation of imidazole **10** under the reaction conditions indicates that radical **12** is not stable and fragments by C–N scission. This mechanistic hypothesis is further supported by the experimental observation that treatment of imidazolium iodide **4** with one-electron reducing agent KC_8 leads directly to the formation of **10** (Figure S4). The radical fragmentation releases an aryl radical that can abstract a second hydrogen atom from **11**. This reaction step then leads to the formation of the dimer **8** and 1,3-di(isopropyl)benzene, the formation of which was experimentally secured by spiking the reaction solution with an authentic sample and analyzing it by ^{1}H NMR spectroscopy (Figure S3).

Dimer **8** constitutes a rare example of a conjugated bis-quinodimethane. For the related Wittig hydrocarbon and the parent bis(*p*-xylylene), which has been prepared in noble-gas matrices at cryogenic temperatures, a diradical character was discussed.[19] This prompted us to investigate the electronic properties of **8** in more detail. To assess the diradical character, we determined the singlet–triplet gap of **8** computationally at the ωB97X-D4/def2-QZVPP/PBEh-3c level of theory. The calculations show that **8** indeed has a remarkably small singlet–triplet gap of only $\Delta E_{S\rightarrow T} =$ 4.4 kcal mol^{-1}. This small energy gap and the intense blue color of **8** in solution indicate possible excitation with visible light. Therefore, we recorded UV/Vis absorption spectra at different concentrations of **8** in THF (Figure 6). We observed an intense absorption band over the entire visible range (400–800 nm) with a maximum at 650 nm ($\varepsilon = 3.8(3)\cdot10^4$ cm^{-1}M^{-1}). Analogous to **1**, this is assigned to a HOMO→LUMO transition corresponding to a π→π* excitation, for which an absorption at 581 nm was computed at

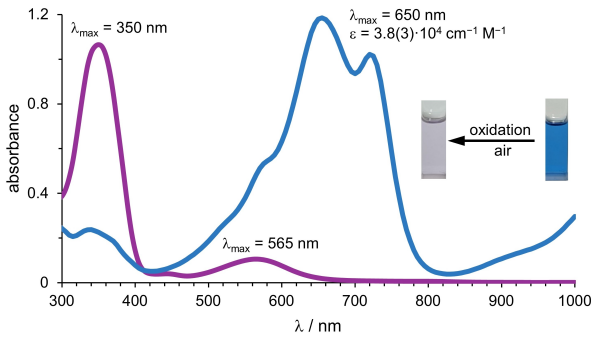

Figure 6. UV/Vis spectrum of **8** in THF (blue, $4\cdot10^{-5}$ mol/L). Upon placing the unmodified sample onto a bench, the color changes from blue to fade purple within minutes due to oxidation (purple).

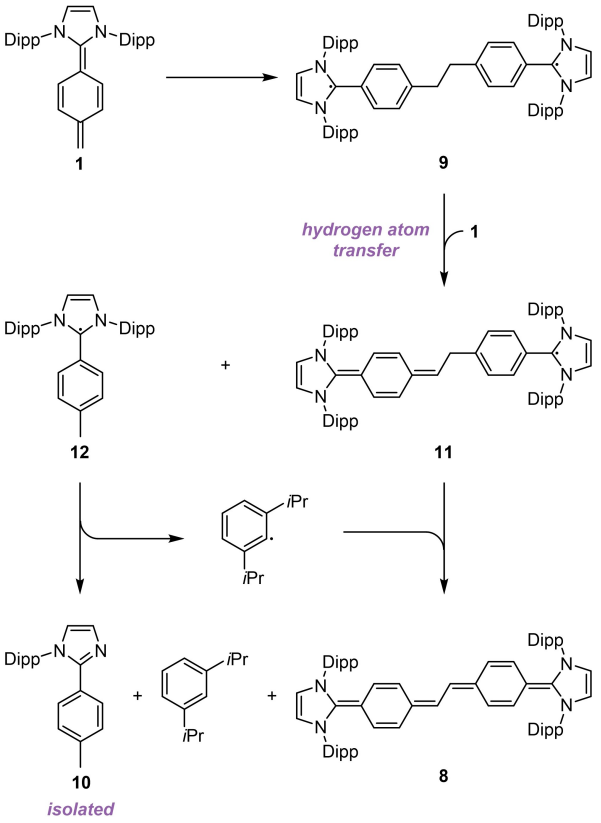

Scheme 7. Proposed mechanism for the formation of **8** and imidazole **10** by a sequence of C–C coupling, hydrogen atom transfer, and radical fragmentation.

the ωB97X-D4/def2-TZVPP//PBEh-3c level by TD-DFT. The bathochromic shift of 320 nm and the greater intensity compared to **1** is likely caused by the extension of π-conjugation in **8** that lowers the HOMO–LUMO gap from 7.0 eV (**1**) to 5.0 eV (**8**). Exposure of **8** to air results in immediate color change from blue to purple. The oxidized species exhibits a broad band in the visible area with low intensity (565 nm) and an intense absorption in the UV region at 350 nm.

We assume that re-aromatization of the two quinoidal rings causes the facile oxidation of **8**. Consequently, we expect a sizeable reducing power from **8** driven by re-aromatization of the entire π-system. To elucidate the redox reactivity of **8** further, we oxidized **8** chemically with two equivalents $AgBF_4$ to obtain the dication **13** in 79 % yield, which was then used to study the redox reactivity of **8** by cyclic voltammetry (Figure 7). We observed a reversible redox event at $E_{1/2} = -1.71$ V (vs Fc/Fc^+) with constant anodic and cathodic peak potentials at scan rates of 50–500 mV/s (Figure S11). These results indicate that **8** is indeed a strong organic electron donor.[20]

Conclusion

In summary, we have prepared an NHQ and documented its dual reactivity: In its closed-shell form, it acts as a

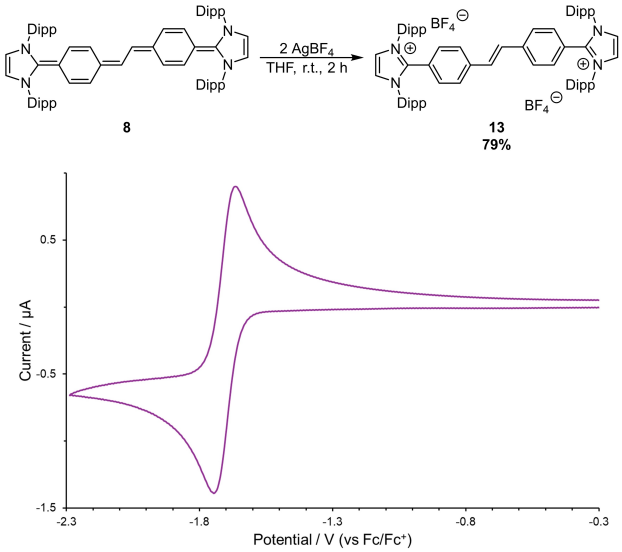

Figure 7. Oxidation of **8** with two equivalents $AgBF_4$ to afford **13** and its cyclic voltammogram ($E_{1/2} = -1.71$ V (vs Fc/Fc^+), 250 mV/s, CH_3CN (0.1 M nBu_4NPF_6)).

comparatively strong organic base with a proton affinity exceeding that of analogous NHCs and NHOs. However, it also exhibits diradical reactivity, as demonstrated by its head-to-head dimerization via an open-shell singlet pathway. This dimerization provides facile access to a conjugated *N*-heterocyclic bis-quinodimethane, which has a small singlet–triplet gap and is a potent organic electron donor. In summary, the present work describes a system that complements the repertoire of strong organic σ-donors with a representative that exhibits radical reactivity. We anticipate that the results presented here will stimulate the development of novel organic σ-donors that enable previously elusive transformations by unlocking radical pathways.

Acknowledgements

This work was supported by the German research foundation (DFG, GE 3117/1-1 and GE 3117/1-2). We thank Dr. H. Hausmann for assistance with NMR experiments and A. Danho, C. E. Campi, and S. Kunz for support with the CV measurements. Prof. P. R. Schreiner, Prof. R. Göttlich, and Prof. H. A. Wegner are acknowledged for their continuous support. Open Access funding enabled and organized by Projekt DEAL.

Conflict of Interest

The authors declare no conflict of interest.

Data Availability Statement

The data that support the findings of this study are available in the supplementary material of this article.

Keywords: DFT Computation · Dimerization · Diradical · Lewis Base · *N*-Heterocyclic Quinodimethane

[1] a) A. J. Arduengo, R. L. Harlow, M. Kline, *J. Am. Chem. Soc.* **1991**, *113*, 361; b) D. Enders, O. Niemeier, A. Henseler, *Chem. Rev.* **2007**, *107*, 5606; c) M. N. Hopkinson, C. Richter, M. Schedler, F. Glorius, *Nature* **2014**, *510*, 485.

[2] a) N. Kuhn, A. Abu-Rayyan, A. Al-Sheikh, K. Eichele, C. Maichle-Mößmer, M. Steimann, Sweidan, *Z. Naturforsch. B* **2005**, *60*, 294; b) N. Kuhn, H. Bohnen, D. Bläser, R. Boese, *Chem. Ber.* **1994**, *127*, 1405; c) N. Kuhn, H. Bohnen, J. Kreutzberg, D. Bläser, R. Boese, *J. Chem. Soc. Chem. Commun.* **1993**, 1136; d) N. Kuhna, H. Bohnena, G. Henkel, J. Kreutzberg, *Z. Naturforsch. B* **1996**, *51*, 1267.

[3] a) A. Fürstner, M. Alcarazo, R. Goddard, C. W. Lehmann, *Angew. Chem. Int. Ed.* **2008**, *47*, 3210; b) K. Powers, C. Hering-Junghans, R. McDonald, M. J. Ferguson, E. Rivard, *Polyhedron* **2016**, *108*, 8; c) B. Maji, M. Horn, H. Mayr, *Angew. Chem. Int. Ed.* **2012**, *51*, 6231.

[4] a) M. M. Hansmann, P. W. Antoni, H. Pesch, *Angew. Chem. Int. Ed.* **2020**, *59*, 5782; b) A. Eitzinger, J. Reitz, P. W. Antoni, H. Mayr, A. R. Ofial, M. M. Hansmann, *Angew. Chem. Int. Ed.* **2023**, *62*, e202309790.

[5] a) S. M. I. Al-Rafia, A. C. Malcolm, S. K. Liew, M. J. Ferguson, R. McDonald, E. Rivard, *Chem. Commun.* **2011**, *47*, 6987; b) A. Causero, H. Elsen, J. Pahl, S. Harder, *Angew. Chem. Int. Ed.* **2017**, *56*, 6906; c) Y. Wang, M. Y. Abraham, R. J. Gilliard, D. R. Sexton, P. Wei, G. H. Robinson, *Organometallics* **2013**, *32*, 6639; d) S. M. I. Al-Rafia, M. J. Ferguson, E. Rivard, *Inorg. Chem.* **2011**, *50*, 10543; e) A. Dumrath, X.-F. Wu, H. Neumann, A. Spannenberg, R. Jackstell, M. Beller, *Angew. Chem. Int. Ed.* **2010**, *49*, 8988; f) I. C. Watson, A. Schumann, H. Yu, E. C. Davy, R. McDonald, M. J. Ferguson, C. Hering-Junghans, E. Rivard, *Chem. Eur. J.* **2019**, *25*, 9678; g) A. Doddi, M. Peters, M. Tamm, *Chem. Rev.* **2019**, *119*, 6994.

[6] a) M. Blümel, R. D. Crocker, J. B. Harper, D. Enders, T. V. Nguyen, *Chem. Commun.* **2016**, *52*, 7958; b) U. Kaya, U. P. N. Tran, D. Enders, J. Ho, T. V. Nguyen, *Org. Lett.* **2017**, *19*, 1398; c) S. Naumann, A. W. Thomas, A. P. Dove, *Angew. Chem. Int. Ed.* **2015**, *54*, 9550; d) H. Wang, Q. Wang, J. He, Y. Zhang, *Polym. Chem.* **2019**, *10*, 3597; e) P. Walther, A. Krauß, S. Naumann, *Angew. Chem. Int. Ed.* **2019**, *58*, 10737.

[7] a) Y.-B. Wang, Y.-M. Wang, W.-Z. Zhang, X.-B. Lu, *J. Am. Chem. Soc.* **2013**, *135*, 11996; b) V. B. Saptal, B. M. Bhanage, *ChemSusChem* **2016**, *9*, 1980; c) W. Li, N. Yang, Y. Lyu, *J. Org. Chem.* **2016**, *81*, 5303; d) L. Y. M. Eymann, P. Varava, A. M. Shved, B. F. E. Curchod, Y. Liu, O. M. Planes, A. Sienkiewicz, R. Scopelliti, F. Fadaei Tirani, K. Severin, *J. Am. Chem. Soc.* **2019**, *141*, 17112; e) P. Varava, Z. Dong, R. Scopelliti, F. Fadaei-Tirani, K. Severin, *Nat. Chem.* **2021**, *13*, 1055; f) P. W. Antoni, C. Golz, J. J. Holstein, D. A. Pantazis, M. M. Hansmann, *Nat. Chem.* **2021**, *13*, 587.

[8] Z. Pei, N. L. Magann, M. J. Sowden, R. B. Murphy, M. G. Gardiner, M. S. Sherburn, M. L. Coote, *J. Am. Chem. Soc.* **2023**, *145*, 16037.

[9] a) D. Rottschäfer, B. Neumann, H.-G. Stammler, M. van Gastel, D. M. Andrada, R. S. Ghadwal, *Angew. Chem. Int. Ed.* **2018**, *57*, 4765; b) D. Rottschäfer, N. K. T. Ho, B. Neumann, H.-G. Stammler, M. van Gastel, D. M. Andrada, R. S. Ghadwal, *Angew. Chem. Int. Ed.* **2018**, *57*, 5838; c) R. S. Ghadwal, *Angew. Chem. Int. Ed.* **2023**, *62*, e202304665.

[10] a) J.-D. Chai, M. Head-Gordon, *J. Chem. Phys.* **2008**, *128*, 84106; b) M. Müller, A. Hansen, S. Grimme, *J. Chem. Phys.* **2023**, *158*, 14103; c) E. Caldeweyher, S. Ehlert, A. Hansen, H. Neugebauer, S. Spicher, C. Bannwarth, S. Grimme, *J. Chem. Phys.* **2019**, *150*, 154122; d) E. Caldeweyher, C. Bannwarth, S. Grimme, *J. Chem. Phys.* **2017**, *147*, 34112.

[11] S. Grimme, J. G. Brandenburg, C. Bannwarth, A. Hansen, *J. Chem. Phys.* **2015**, *143*, 54107.

[12] a) H. Song, E. Lee, *Chem. Eur. J.* **2023**, *29*, e202203364; b) K. C. Mondal, P. P. Samuel, H. W. Roesky, B. Niepötter, R. Herbst-Irmer, D. Stalke, F. Ehret, W. Kaim, B. Maity, D. Koley, *Chem. Eur. J.* **2014**, *20*, 9240; c) R. Gompper, H.-U. Wagner, E. Kutter, *Chem. Ber.* **1968**, *101*, 4144; d) F. Witte, P. Rietsch, S. Sinha, A. Krappe, J.-O. Joswig, J. P. Götze, N. Nirmalananthan-Budau, U. Resch-Genger, S. Eigler, B. Paulus, *J. Phys. Chem. B* **2021**, *125*, 4438; e) P. Srujana, T. Gera, T. P. Radhakrishnan, *J. Mater. Chem. C* **2016**, *4*, 6510.

[13] R. S. Ghadwal, S. O. Reichmann, R. Herbst-Irmer, *Chem. Eur. J.* **2015**, *21*, 4247.

[14] W. S. Trahanovsky, S. P. Lorimor, *J. Org. Chem.* **2006**, *71*, 1784.

[15] Deposition numbers 2304290 (for **6**), and 2304291 (for **8**) contain the supplementary crystallographic data for this paper. These data are provided free of charge by the joint Cambridge Crystallographic Data Centre and Fachinformationszentrum Karlsruhe Access Structures service.

[16] a) Y. Ito, S. Miyata, M. Nakatsuka, T. Saegusa, *J. Org. Chem.* **1981**, *46*, 1043; b) L. A. Errede, R. S. Gregorian, J. M. Hoyt, *J. Am. Chem. Soc.* **1960**, *82*, 5218.

[17] a) K. Oyaizu, K. Saito, E. Tsuchida, *Chem. Lett.* **2000**, *29*, 1318; b) Y. Liu, P. Varava, A. Fabrizio, L. Y. M. Eymann, A. G. Tskhovrebov, O. M. Planes, E. Solari, F. Fadaei-Tirani, R. Scopelliti, A. Sienkiewicz, C. Corminboeuf, K. Severin, *Chem. Sci.* **2019**, *10*, 5719.

[18] A. V. Marenich, C. J. Cramer, D. G. Truhlar, *J. Phys. Chem. B* **2009**, *113*, 6378.

[19] a) G. Wittig, B. Fartmann, *Justus Liebigs Ann. Chem.* **1943**, *554*, 213; b) R. Marquardt, W. Sander, T. Laue, H. Hopf, *Liebigs Ann. Recl.* **1996**, *1996*, 2039; c) D. Henseler, G. Hohlneicher, *J. Mol. Struct.* **1999**, *480–481*, 515.

[20] a) J. A. Murphy, *J. Org. Chem.* **2014**, *79*, 3731; b) H. S. Farwaha, G. Bucher, J. A. Murphy, *Org. Biomol. Chem.* **2013**, *11*, 8073; c) E. Doni, J. A. Murphy, *Chem. Commun.* **2014**, *50*, 6073.

Manuscript received: November 3, 2023
Accepted manuscript online: December 13, 2023
Version of record online: January 18, 2024